FEBS Letters 585 (2011) 3348–3353

journal homepage: www.FEBSLetters.org

Identification of a unique splicing regulatory cluster in hepatitis B virus pregenomic RNA

Joydip Bhanja Chowdhury, Dipika Roy, Sagarmoy Ghosh *

Department of Microbiology, University of Calcutta, University College of Science and Technology, 35 Ballygunge Circular Road, Kolkata 700 019, India

ARTICLE INFO

Article history:
Received 12 July 2011
Revised 10 September 2011
Accepted 19 September 2011
Available online 29 September 2011

Edited by Hans-Dieter Klenk

Keywords:
Splicing
HBV
ISS
HBSP
Intronic splicing activator

ABSTRACT

HBV particles with genome derived from spliced mRNAs accumulate in patients with virus-derived severe liver necrosis and fibrosis. We investigated the role of an intronic element (intronic splicing silencer-long, ISS_L) on splicing of HBV minigene transcripts. Removal of the entire ISS_L showed two-fold increase in splicing while shorter deletions within ISS_L indicated isolated clusters of activator and repressor domains. Activator domains stimulated splicing in presence of PRE, a long HBV 3′ exon and even when present in a heterologous context. Mutations in the repressor domain unexpectedly augmented repression. The role of this intronic splicing regulatory element could be important for HBV pathogenesis.

1. Introduction

Hepatitis B virus (HBV), a member of the hepadnaviridae family, is a 42 nm particle with an enveloped 28 nm nucleocapsid. Transcription on the HBV genome by host RNA polymerase II produces 3′-coterminal pregenomic/precore RNA (pgRNA, 3.5 kb) and three subgenomic RNAs (2.4, 2.1 and 0.8 kb) [1]. Individual promoters and related enhancer elements that are regulated by ubiquitous or liver enriched transcription factors, drive transcription of these viral RNAs [2].

Splicing of viral transcripts in hepadnaviridiae family has diverse effects in viral life cycle. Replication of duck hepatitis B virus (DHBV) in infected primary duck hepatocytes and ducks requires a spliced mRNA [3]. Even though no direct role of splicing could be established for HBV replication [4], the load of defective HBV particles with shortened genome increased with liver necroinflammation and fibrosis [5]. In cultured hepatocytes, about 50% DNA within intracellular capsids is derived from spliced RNAs [6]. In patient sera and HBV infected cultured hepatocytes, eleven smaller than full-length genomes are generated from spliced pgRNA [7,8]. Of these spliced RNAs, two products (SP1 and SP2) predominate. The SP1 product is obtained by removal of intron with 5′ donor and 3′ acceptor sites positioned at 2447nt and 489nt, respectively, but generation of SP2 requires the donor at 2067nt and the same acceptor site. The search for *cis*- and *trans*-acting factors regulating pgRNA splicing has identified both activator and repressor regions in Post-transcriptional Regulatory Element (PRE) present in the 3′ exon of pgRNA [9]. Recently a double-hairpin structure in PRE, when placed in a heterologous intron, silenced splicing in a structure and position-dependent fashion [10]. However effect of HBV intronic elements in splicing of a homologous transcript has never been reported.

At least two proteins encoded by spliced HBV RNAs are found in patient sera and cultured hepatocytes. An endoglycosylase H (endo-H) sensitive 43 kDa polymerase-surface fusion protein translated from a HBV spliced RNA was reported in cells expressing HBV P protein. HBSP, encoded by a 2.2 kb singly spliced mRNA generated by the same splice sites used for generating SP1 species [11], bound to the fibrinogen γ-chain and inhibited fibrin formation [12]. Taken together the role of splicing in HBV infection remains a very crucial unanswered question.

To gain insight of how intronic splicing signals dictate splicing in HBV, we investigated the role of an intronic element (intronic splicing silencer-long, ISS_L) with a pronounced secondary structure in homologous minigene context. The minigene transcript is very similar to the HBSP pre-mRNA and thus should recapitulate the events leading to its processing. Our data reveal that the ISS_L is actually composed of interspersed repressor and activator domains. The activator domains could stimulate splicing even when

Abbreviations: HBV, hepatitis B Virus; pgRNA, pregenomic RNA; ISS_L, intronic splicing silencer-long; PRE, post transcriptional regulatory element; HBSP, hepatitis B splice-generated protein; RT-PCR, reverse transcriptase-polymerase chain reaction

* Corresponding author. Fax: +91 33 2461 4849.
E-mail address: sgmicrobio@caluniv.ac.in (S. Ghosh).

0014-5793/$36.00
doi:10.1016/j.febslet.2011.09.026

the 3′ exon harbored PRE or the almost entire length of HBV 3′ exon. Moreover these activator domains were also functional in a heterologous pre-mRNA. A separate repressor motif within the intron was also identified. To our knowledge this is the first report of *cis*-acting intronic splicing regulators from HBV RNA.

2. Materials and methods

2.1. Cell lines and oligonucleotides

HuH7 cell line was maintained in Dulbecco's modified Eagle's medium with 10% fetal bovine serum. The primers used in cloning and PCR are depicted in Supplementary Table 1.

2.2. Preparation of minigene constructs

Different regions of the HBV genome were amplified from a plasmid containing the entire HBV sequence (NCBI No. AY945307) and cloned in pcDNA 3.1(+) expression vector (Invitrogen) under CMV-IE promoter. CPS, the basal construct contained sequences spanning 2231–3182 bp followed by 20–621 bp of HBV genome to include the nucleotide positions 2447 and 489 as splice donor and acceptor sites with a 1204nt intron separating them. CPS and CPSISS$_L$ΔISR1 backgrounds were used for PCR with mutagenic primers to generate ISS$_L^M$ mutants. PRE (1151–1684nt) and 3′ exonic region of pgRNA (622–1800nt) were inserted downstream of CPS by EcoRI and KpnI sites to construct CPSPRE and CPSpg minigenes respectively. For reporter assays using pCI-neo mammalian expression vector (Promega), respective primer pairs were annealed (Supplementary Table I), and inserted into the intron present in the vector backbone. All the constructs were confirmed by DNA sequencing.

2.3. Transfection

Transient transfections were performed in 6-well plates by $CaCl_2$ using standard protocols. Each well typically received a mixture of 2 μg of test plasmid, 1 μg of pEGFP-C1 (Clontech), and 2 μg of pUC19. Total RNA was isolated 48 hours post-transfection using TRI reagent (Sigma) following manufacturer's instructions.

2.4. Semiquantitative determination of transcripts

Reverse transcription of isolated total RNA was done with random hexamers. Hp8 and Hp2 primer pair was used for amplification of cDNA from precursor RNA and Hp1 and Hp2 pair was used for amplification of cDNA from spliced RNA. Serial 10-fold dilutions of target RNA was simultaneously assayed alongside the cellular RNAs to ascertain that the amplification of the products was on the exponential phase. Each RNA sample was normalized with respect to GFP and GAPDH transcripts. All the tubes were simultaneously PCR amplified with [α-^{32}P]dCTP and analyzed in 6% nondenaturing polyacrylamide gel. To compare the band intensities across multiple gels, all the gels under analysis were exposed together to a phosphorimager screen and analyzed by ImageQuant TL software. Splicing efficiency was calculated as [pixel value of spliced/pixel values of (spliced + unspliced)] for each sample.

Splicing in pCI-neo background was assayed with pCIF and pCIR primer pair that amplifies both spliced (161 bp) and unspliced (293 bp for pCI-neo transcript and 313 bp for pCI-neo + 20nt insert transcript) species.

2.5. Real-time RT-PCR

After reverse transcription, cDNA was amplified in StepOnePlus™ real-time PCR System (Applied Biosystems) using Maxima™ SYBR Green/ROX qPCR Master Mix(2×) (Fermentas) and specific primers. HpRT1 and HpRT2 primer pair was used for amplification of cDNA from spliced species and HpRT11 and HpRT2 pair was used for amplification of total minigene cDNA. For standard curves of C_t vs. log[RNA in ng], two step RT-PCR was performed on known amounts of in vitro transcribed target RNA. The relative quantities of spliced or total RNA in each sample under investigation were obtained from the respective standard curves. Data shown here represents mean of at least three independent experiments with error bar representing ±standard deviation. Student's *t*-test was performed with GraphPad Prism 5 software.

2.6. RNA stability assay

Twenty-four hours post transfection, cells were treated with 1 μg/ml Actinomycin D and kept at 37 °C for indicated time and total RNA was extracted. The isolated RNA was analyzed by phosphorimager quantitation as described above. RNA levels were normalized against GAPDH mRNA.

3. Results and discussion

3.1. The HBV intron contains a splicing silencer

To establish an in vitro system that recapitulates the splicing regulation of HBV pre-mRNA, we designed minigenes under the control of CMV-IE promoter and transfected them into HuH7 human hepatocarcinoma cell line. The CMV-IE promoter has been shown to enhance the accumulation of spliced transcripts for retroviral genes when compared to their endogenous promoters and also for HBV where the combination of both CMV-IE promoter and HuH7 cells as transfection hosts were noted to produce more splice variant RNA [13]. We constructed a basal minigene (CPS, as it includes regions from these three HBV genes) to recapitulate splicing of HBV major spliced product SP1 and the HBSP mRNA (Fig. 1). Both semiquantitative radioactive RT-PCR and real-time RT-PCR analyses were carried out to elucidate the level of splicing of the transcripts. We explored the secondary structure of the intron of the minigene with MFOLD (http://www.bioinfo.rpi.edu/applications/mfold) using default settings to give us idea about the presence of structured regulatory motifs [14]. We concentrated on an element spanning 2951–3163nt that was conserved in all the predicted structural conformations of HBV intron in different free

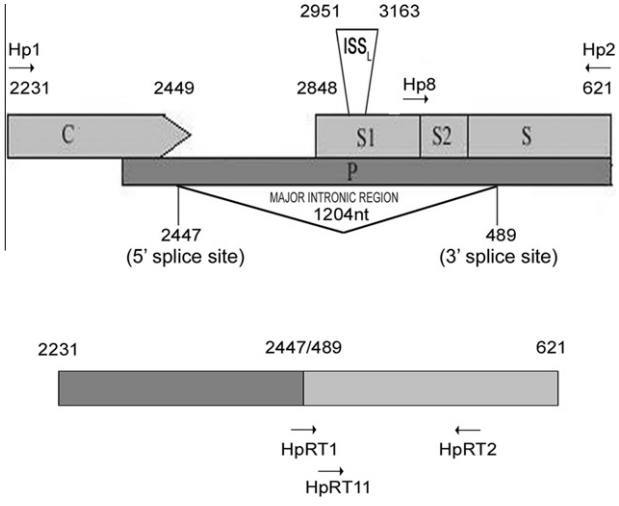

Fig. 1. Construction of the basal minigene, CPS. The 5′ and 3′-splice sites in pgRNA and their positions in HBV genes are indicated. ISS$_L$ was deleted from CPS (CPSΔISS$_L$), when indicated (upper panel). Arrows show location of the primers used for amplification of cDNA. Primers for real-time PCR for identification of spliced and total minigene transcripts are shown in lower panel.

energy levels. The region showed extensive base-pairing between both contiguous and distal sequences and formation of alternative structural conformers seemed possible (Fig. 2). We posited that formation of such alternative conformers could be linked to regulation of pgRNA maturation and investigated whether splicing of the transcribed pre-mRNA in transfected HuH7 cells was affected by deletion of this structure from the minigene construct.

Real-time PCR analysis of the expressed RNA revealed that deletion of this structured motif doubled the level of spliced RNA when compared to CPS indicating presence of a splicing repressor domain (Fig. 3A). As a complementary approach we looked directly at the level of spliced and unspliced minigene transcripts by semiquantitative RT-PCR followed by phosphorimaging (Fig. 3B). Increase in the level of spliced products in deletion mutants further reinforced our real-time RT-PCR observation. Accordingly we termed this structured region as ISS_L (intronic splicing silencer-long).

3.2. ISS_L has separate activator and repressor domains

The increase in splicing upon deletion of ISS_L led us to further investigate the role of different sequence elements within it. We progressively removed 20nt fragments from the 5′end starting from 2951nt (Fig. 4A, upper panel) or specific 20nt fragments (lower panel). Our data indicated that the effect of ISS_L is actually bipartite and it contains both splicing activator and inhibitor domains (Fig. 4B). Deletion of first 20nt from the 5′ end of ISS_L inhibited splicing to 10% of CPS implying its role as a splicing activator. Deletion of next 20nt region on the other hand rescued splicing to almost the same level of CPS. Further deletions upto 100nt from the 5′ end of ISS_L (2951–3050nt of HBV) did not significantly alter the level of splicing. But deletion of immediate downstream sequence ($CPSISS_L\Delta$2951–3070) abruptly caused the splicing to diminish to almost an undetectable level. However further downstream deletions in ISS_L rescued inhibition. We named these intronic splicing activators as ISA1 (2951–2970nt) and ISA2 (3051–3070nt) respectively. Removal of sequences in the 3′ end of ISS_L significantly increased splicing (compare $CPSISS_L\Delta$2951–3130 with $CPS\Delta ISS_L$) implying that the 3131–3163nt of HBV harbors a splicing silencer. Taken together our results indicate that the splicing repressor and activator domains are distinct and scattered throughout ISS_L.

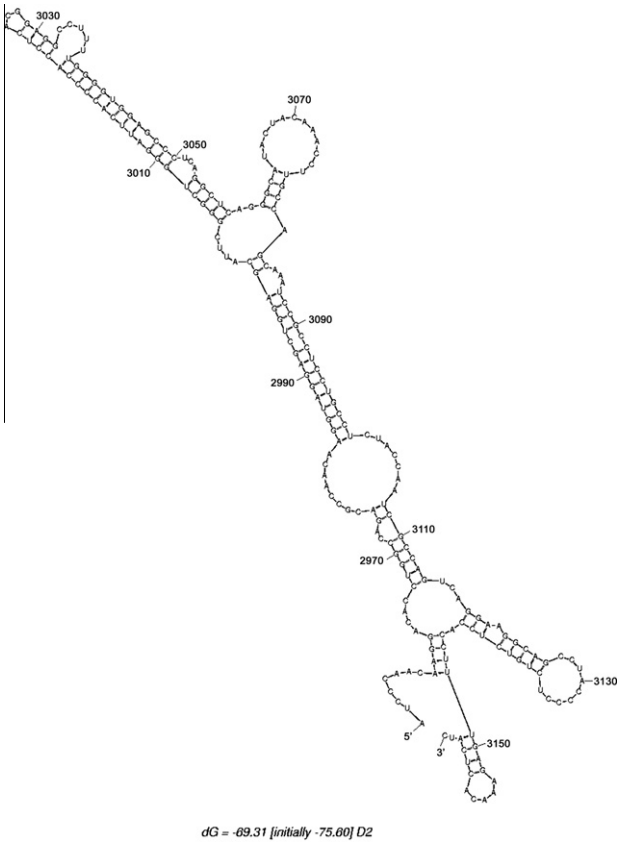

Fig. 2. MFOLD generated secondary structure of ISS_L. Note extensive base-pairing within the region resulting in juxtaposition of distal sequences.

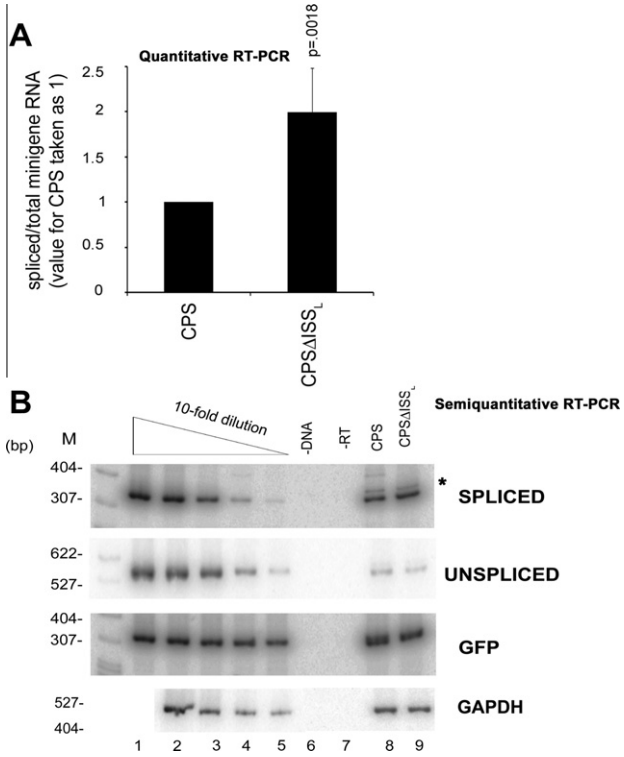

Fig. 3. Splicing profile of CPS and its deletion construct. (A) Removal of ISS_L favors splicing. Quantitative RT-PCR analysis shows two-fold splicing repression by ISS_L. All results are representative of minimum three independently performed experiments. The histogram shows mean ± standard deviation. (B) Direct visualization of spliced and total minigene transcripts also demonstrate enhanced splicing in $CPS\Delta ISS_L$. The asterisk indicates a minor spliced product SP3 that utilizes a weak 5′-ss at 2471. In lanes 1–5, 10-fold decreasing amounts of target RNA were analyzed.

To further characterize the role of these individual elements in ISS_L we deleted individual 20nt elements within ISS_L (Fig. 4C). While deletion of ISA1 and ISA2 regions were sufficient to repress, specific deletions of 3111–3130nt (ISR1) and 3131–3163nt (ISR2) did not affect splicing appreciably. It is pertinent to note that removal of 3111–3163nt terminal region in ISS_L activates splicing in absence of rest of ISS_L but their specific removal does not have any significant effect. This possibly means that the terminal repressor is squelched by rest of the sequence in ISS_L by some unknown mechanism.

3.3. Activator domains are still active in presence of PRE, long HBV exon and in a heterologous context

Addition of PRE (CPSPRE) or almost entire 3′ exon of SP1 (CPSpg) downstream of CPS suppressed the level of splicing. Removal of ISA1 or ISA2 in these backgrounds further diminished splicing efficiencies. In $CPSPRE\Delta ISA1$ and $CPSPRE\Delta ISA2$ transcripts, splicing was reduced to 30% and 7%, respectively compared to CPS (Fig. 5A), while that in $CPSpg\Delta ISA1$ and $CPSpg\Delta ISA2$ were 10% and 17%, respectively (Fig. 5B). Therefore ISA1 and ISA2 activate splicing in the presence of exonic sequences known to harbor other splicing regulators.

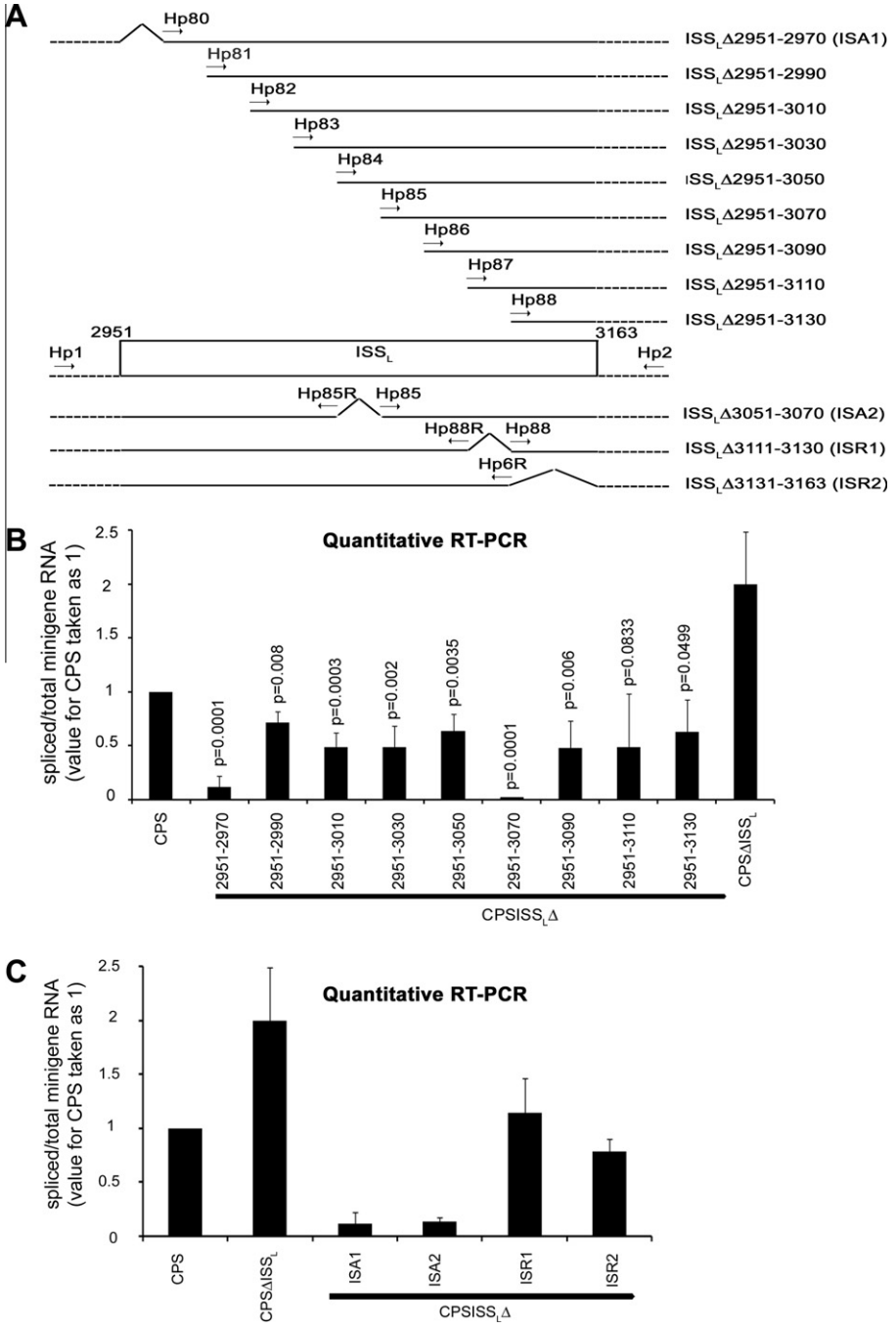

Fig. 4. (A) Progressive deletions in ISS$_L$. (A) Schematic of deletion constructs. A fixed 5′-half of the CPS was ligated to progressively truncated fragments of ISS$_L$ (ISS$_L$Δ2951–2970 to ISS$_L$Δ2951–3130). Lower panel shows schematic of specific 20 bp deletion constructs. Locations of conjugate primer pairs for specific 20 bp deletions in ISS$_L$ are indicated. (B) Real-time RT-PCR analysis showing deletion of 2951–2970nt and 3051–3070nt (ISA1 and ISA2) repressed splicing to 10% of basal minigene. Removal of 3131–3163nt in ISS$_L$ showed maximum stimulation of splicing. (C) Real-time RT-PCR demonstrates splicing activation associated with ISA1 and ISA2. Deletion of only ISR1 or ISR2 marginally affected splicing.

Insertion of ISA1 and ISA2 in the intron of pCI-neo increased splicing by 3-fold and 7-fold, respectively, as revealed by semi-quantitative analysis (data not shown), implying a generalized splicing activator function even in a heterologus context. We also ascertained that the stability of either the precursor or the spliced RNA from different minigenes were similar (Fig. 5C).

3.4. Mutations interfere with 3′ terminal repressor function

Intramolecular base-pairing between ISR1 and ISR2 suggests an internal stem-loop structure (Fig. 6A). In this conformation, a stem-loop could form between two neighboring regions, 3118–3126nt (GGAAGGCAG) and 3136–3143nt (CUGUCUCC). To investigate whether formation of such stem is important for repression of splicing, we mutated ISR2 (3138–3143nt; GUCUCC to UGUAGU) to abolish interaction with ISR1. Our results demonstrate that mutation in these sequences (ISS$_L^M$CPS) actually augmented repression irrespective of presence of ISR1 (Fig. 6B). Therefore 3138–3143nt (GUCUCC) in ISR2 plays a crucial role in regulation of splicing in HBV.

The interspersed presence of regulatory domains within ISS$_L$ raises interesting possibilities. Firstly, ISA1 and ISA2 were immedi-

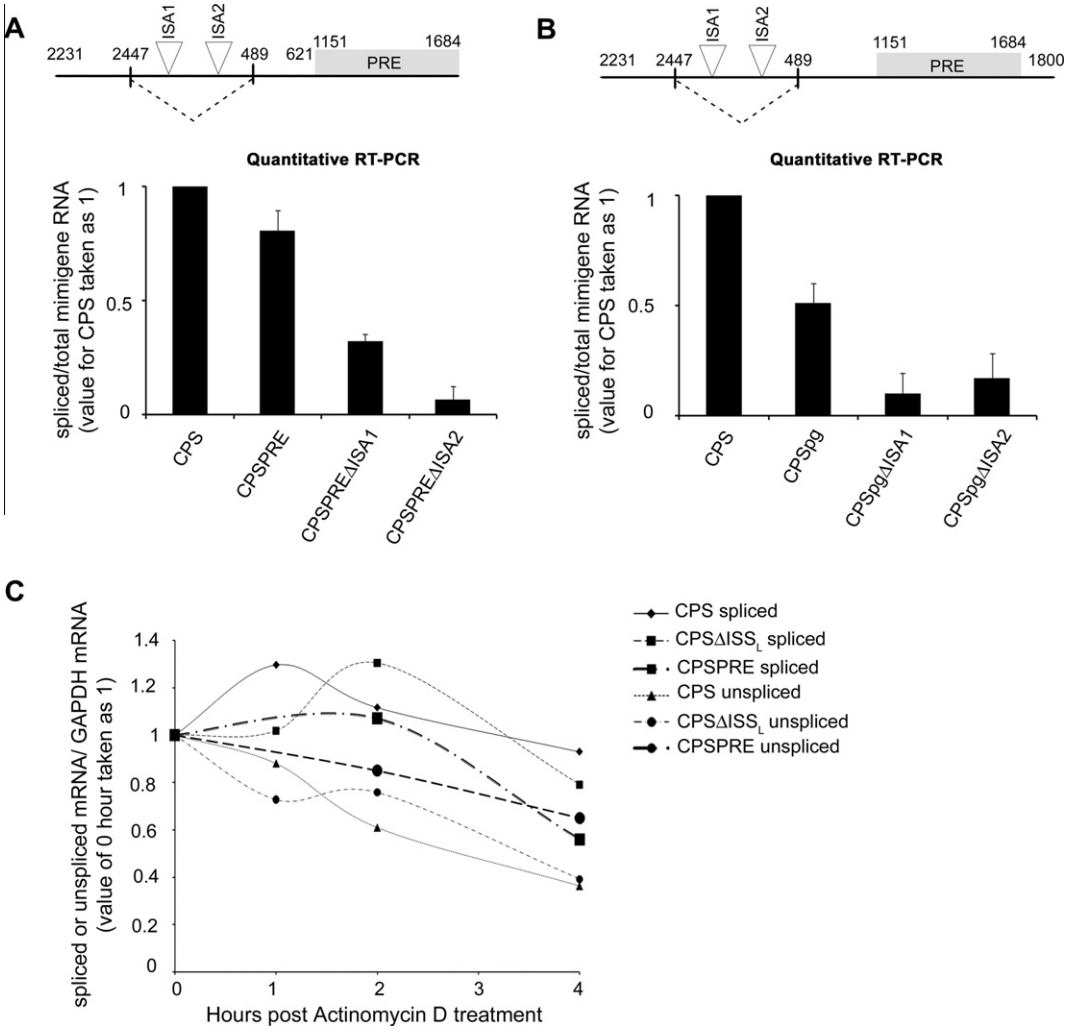

Fig. 5. Analysis of splicing activation by ISA1 and ISA2. Real-time RT-PCR shows deletion of either ISA1 or ISA2 in CPSPRE (A) or CPSpg (B) drastically reduces splicing. (C) The stability of the spliced and precursor RNA of different minigenes were similar following treatment with 1 μg/ml Actinomycin D for indicated times.

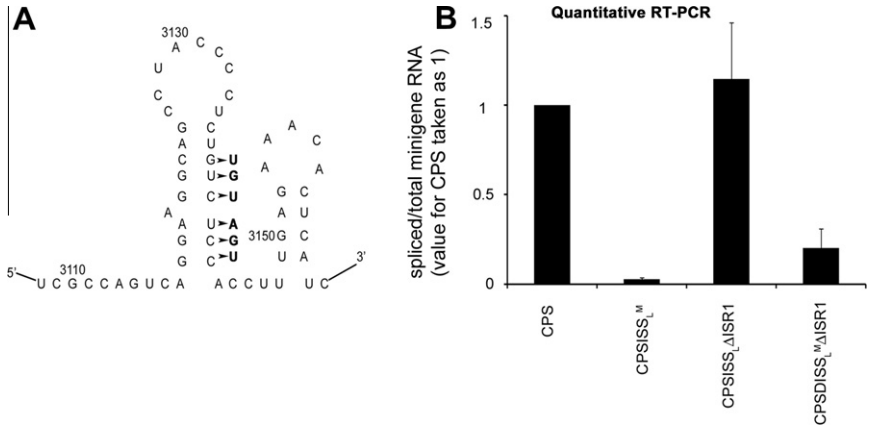

Fig. 6. Mutation analysis of repressor domain. (A) ISR1 and ISR2 can form a stem-loop structure. The mutations (UGUAGU in bold) that disrupt such structure in ISS$_L^M$CPS are shown. (B) Real-time RT-PCR analysis shows mutation of 3138–3143nt (GUCUCC to UGUAGU) results in strong repression of splicing in CPS and ΔISR1 constructs.

ately followed by repressor domains (Fig. 4B) and their interaction could possibly determine the fate of pgRNA transcripts depending on cognate cellular signals. The ability of ISA1 and ISA2 to activate splicing in presence of PRE or the entire 3′ exon and even in a heterologous pre-mRNA indicates independent activator function. Secondly, mutation of 3138–3143nt in ISR2 resulted in strong repression of splicing (Fig. 6B). These sequences therefore attenuate repression even being embedded within a repressor element.

4. Conclusion

Our data depicts the presence of an intronic splicing regulator domain in pgRNA with interspersed splicing activator and repressor regions. The two intronic splicing activators, ISA1 and ISA2, can possibly function as general splicing activators. On the other hand, 3138–3143nt in ISR2 possibly attenuates repression. The identification of nuclear factors that recognize the individual RNA elements and their correlation with status of HBV disease pathology remains an important question.

Acknowledgments

We thank Dr. Shaheed Jameel (ICGEB, India) for providing the HuH7 hepatocarcinoma cell line and Dr. Runu Chakravarti (NICED, India) for the plasmid harboring the entire HBV genome. The work is supported by Grant No. 37(1205)/04/EMR-II from CSIR. J.B.C. and D.R. are supported by research fellowship from CSIR and UGC.

Appendix A. Supplementary data

Supplementary data associated with this article can be found, in the online version, at doi:10.1016/j.febslet.2011.09.026.

References

[1] Ganem, D. and Varmus, H.E. (1987) The molecular biology of the hepatitis B viruses. Annu. Rev. Biochem. 56, 651–693.
[2] Quasdorff, M. and Protzer, U. (2010) Control of hepatitis B virus at the level of transcription. J. Viral Hepat. 17, 527–536.
[3] Obert, S., Zachmann-Brand, B., Deindl, E., Tucker, W., Bartenschlager, R. and Schaller, H. (1996) A splice hepadnavirus RNA that is essential for virus replication. EMBO J. 15, 2565–2574.
[4] Park, G.S., Kim, H.Y., Shin, H.S., Park, S., Shin, H.J. and Kim, K. (2008) Modulation of hepatitis B virus replication by expression of polymerase-surface fusion protein through splicing: implications for viral persistence. Virus Res. 136, 166–174.
[5] Soussan, P., Pol, J., Garreau, F., Schneider, V., Le, P.C., Nalpas, B., Lacombe, K., Bonnard, P., Pol, S. and Kremsdorf, D. (2008) Expression of defective hepatitis B virus particles derived from singly spliced RNA is related to liver disease. J. Infect. Dis. 198, 218–225.
[6] Rosmorduc, O., Petit, M.A., Pol, S., Capel, F., Bortolotti, F., Berthelot, P., Brechot, C. and Kremsdorf, D. (1995) In vivo and in vitro expression of defective hepatitis B virus particles generated by spliced hepatitis B virus RNA. Hepatology 22, 10–19.
[7] Gunther, S., Sommer, G., Iwanska, A. and Will, H. (1997) Heterogeneity and common features of defective hepatitis B virus genomes derived from spliced pregenomic RNA. Virology 238, 363–371.
[8] Sommer, G., van, B.F. and Will, H. (2000) Genotype-specific synthesis and secretion of spliced hepatitis B virus genomes in hepatoma cells. Virology 271, 371–381.
[9] Heise, T., Sommer, G., Reumann, K., Meyer, I., Will, H. and Schaal, H. (2006) The hepatitis B virus PRE contains a splicing regulatory element. Nucleic Acids Res. 34, 353–363.
[10] Huang, C., Xie, M.H., Liu, W., Yang, B., Yang, F., Huang, J., Huang, J., Wu, Q., Fu, X.D. and Zhang, Y. (2011) A structured RNA in hepatitis B virus post-transcriptional regulatory element represses alternative splicing in a sequence-independent and position-dependent manner. FEBS J. 278, 1533–1546.
[11] Soussan, P., Garreau, F., Zylberberg, H., Ferray, C., Brechot, C. and Kremsdorf, D. (2000) In vivo expression of a new hepatitis B virus protein encoded by a spliced RNA. J. Clin. Invest. 105, 55–60.
[12] Chen, J.Y., Chen, W.N., Liu, L.L., Lin, W.S., Jiao, B.Y., Wu, Y.L., Lin, J.Y. and Lin, X. (2010) Hepatitis B spliced protein (HBSP) generated by a spliced hepatitis B virus RNA participates in abnormality of fibrin formation and functions by binding to fibrinogen gamma chain. J. Med. Virol. 82, 2019–2026.
[13] Abraham, T.M., Lewellyn, E.B., Haines, K.M. and Loeb, D.D. (2008) Characterization of the contribution of spliced RNAs of hepatitis B virus to DNA synthesis in transfected cultures of Huh7 and HepG2 cells. Virology 379, 30–37.
[14] Zuker, M. (2003) MFOLD web server for nucleic acid folding and hybridization prediction. Nucleic Acids Res. 31, 3406–3415.